

7th HPC 2016 – CIRP Conference on High Performance Cutting

## Influence of Machining Parameters on Heat Generation during Milling of Aluminum Alloys

B. Denkena<sup>a</sup>, J. Brüning<sup>a</sup>, D. Niederwestberg<sup>a</sup>, R. Grabowski<sup>a\*</sup><sup>a</sup> Institute of Production Engineering and Machine Tools, Leibniz Universität Hannover, An der Universität 2, D-30823 Garbsen, Germany\* Corresponding author. Tel.: +49 511/762-18331; fax: +49 511/762-5115. E-mail address: [grabowski@ifw.uni-hannover.de](mailto:grabowski@ifw.uni-hannover.de)

### Abstract

Thin-walled components, i.e. fuselage frames of airplanes, are prone to an unstable process behavior during milling. Therefore, tools with a chamfer between the cutting edge and the flank face are often used for such machining tasks. During milling, the chamfered area comes into contact with the just cut surface. This contact leads to process damping forces and the induced heat into the workpiece in this contact zone is increased. Furthermore, the amount of induced heat depends on the process parameters. At certain spots on the machined surface this may lead to a local overheating, which can reduce stiffness significantly. When this occurs during milling of a thin-walled component, the component is often regarded as reject. In this paper, the influence of chamfers and process parameters on the induced heat into the workpiece is investigated experimentally. In addition, a simulation which predicts the temperature in the workpiece in dependence of the process parameters is presented.

© 2016 Published by Elsevier B.V. This is an open access article under the CC BY-NC-ND license (<http://creativecommons.org/licenses/by-nc-nd/4.0/>).

Peer-review under responsibility of the International Scientific Committee of 7th HPC 2016 in the person of the Conference Chair Prof. Matthias Putz

**Keywords:** thermal behaviour; simulation; milling; process damping

### 1. Introduction

The aircraft manufacturer Airbus forecasts that the worldwide air traffic will double in the next 15 years which leads to a demand of more than 30,000 new aircrafts [1]. Modern aircrafts are designed in order to maximize energy efficiency by low weight. Therefore, the structure components are designed with minimal residual material thickness as low as 1 to 2 mm and maximum rigidity. These complex shaped parts are up to 14 m long and typically manufactured from rolled aluminum plates or near-net-shape extruded aluminum profiles. The chosen materials are difficult to machine and challenging for the machining process like distortions.

Thin-walled workpieces have a high compliance, and thus, compared to more solid workpieces, self-excited vibrations may occur more easily during machining [2]. The dynamic displacement between the tool and the workpiece leads to a variation of the chip thickness and a wavy workpiece surface. This phenomenon is known as the regenerative effect [3]. Andrew and Tobias stated that if with every following cut the amplitude of the chip thickness is increasing due to the

regenerative effect, the machining process becomes unstable [4]. Tools with cutting edges, which have chamfers on their flank face, are used to increase the process stability [5]. This chamfered areas come into contact with the just cut wavy surface of the workpiece leading to an additional force component known as process damping forces [6]. However, this additional contact also has an influence on heat generation. It is to be expected that this is critical for aluminum alloys with increased tendency for soft spots. These thermal induced structural changes of the material texture lead to a reduced stiffness in the border area of the material [7]. Several experimental investigations showed that this effect could occur in cutting processes [8]. For the detailed simulation and analysis of thermal effects in machining processes, the finite difference method is an approved method [9].

### 2. Approach

In this paper, experiments to investigate process stability and heat generation when milling thin-walled workpieces are carried out. An end mill with sharp and chamfered cutting

edges, is examined in order to analyze differences in heat generation and stability due to the different cutting edge shape. The simulation approach is based on a 2D-sectional view of workpiece and process. Therefore the workpiece is sliced horizontal at half cutting depth. For the determination of the heat input an inverse method was used.

### 3. Experimental investigations & simulation

#### 3.1. Experimental setup

For the investigation of the influence of chamfered cutting edges on process stability and heat generation, the setup shown in Fig. 1 is used. The workpiece is a small part of a frame with a thickness of 2 mm. A force plate is used to analyze the cutting forces and process stability respectively. The workpiece material is Al-Li 2196, which is commonly used in aerospace applications. A thermal imaging camera is used to measure the heat development on the backside of the workpiece. For a more accurate temperature measurement, the backside is coated with an emissivity spray.

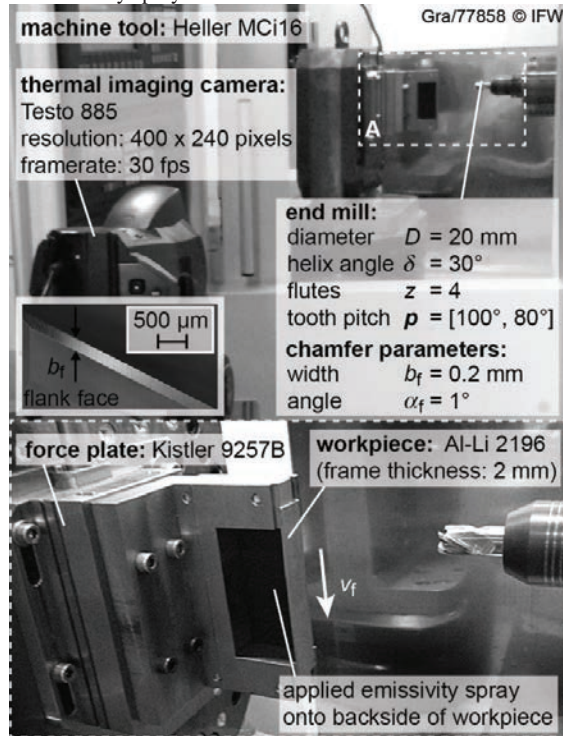


Fig. 1. Experimental configuration

Two similar end mills are used for the experiments. One has sharp cutting edges and the other one has chamfered cutting edges. The chamfer specific values have been chosen based on the experiments by Sellmeier and Denkena [5]. During the milling operation, the axial and radial depth of cut  $a_p$  and  $a_e$ , respectively, have constant values (see Table 1). The spindle speed  $n$  and feed per tooth  $f_z$  were varied to investigate the influence on stability and heat development.

Table 1: Experimental process parameters

process parameter	values
spindle speed $n$	[1,000 ... 10,000] min <sup>-1</sup>
feed per tooth $f_z$	[0.08 ... 0.3] mm
axial depth of cut $a_p$	25 mm
radial depth of cut $a_e$	1 mm
milling direction	down milling
coolant	none

#### 3.2. Simulation

The process is simulated by a finite difference method. For the calculation of the heat flux, the domain of the method was divided into cubic elements with an edge length of the feed per tooth  $f_z$ . Every element of the domain has several properties which can be defined global if they are homogeneous or local if they are inhomogeneous.

Table 2: Element properties of the simulation model

homogeneous properties	inhomogeneous properties
edge length $dx$ [mm]	heat quantity [J]
thermal conductivity $\lambda$ [W/mmK]	material removal [-]
mass $m$ [kg]	temperature $T$ [K]
specific heat capacity $c_p$ [J/kgK]	

The heat flux properties are homogeneous. The domain is discretized cubical. Therefore, the local heat quantity of the elements can be stored as matrix  $Q$ . The local temperature  $T$  can be calculated by the local heat quantity and the specific material properties. An additional matrix  $A$  of identical size is used to model the material removal during the process. This matrix is binary-coded to take into account whether there is material or not (Fig. 2).

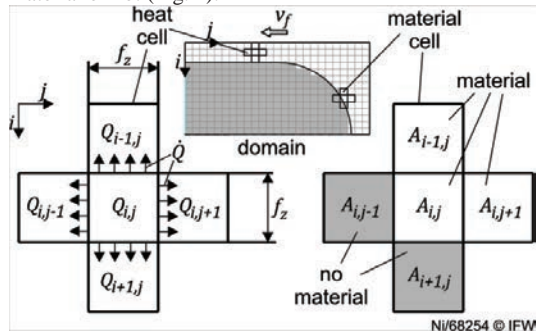


Fig. 2. Domain with single heat and material cell

Based on this description, the heat difference  $\Delta Q_{i,j}$  for every element can be calculated by equation 1. The heat difference is depending on the properties of the neighboring elements and the time of a simulation step  $\Delta t$ .

$$\Delta Q_{i,j} = A_{i,j} \cdot \begin{bmatrix} A_{i-1,j} \\ A_{i+1,j} \\ A_{i,j-1} \\ A_{i,j+1} \end{bmatrix}^T \cdot \begin{pmatrix} Q_{i-1,j} \\ Q_{i+1,j} \\ Q_{i,j-1} \\ Q_{i,j+1} \end{pmatrix} - Q_{i,j} \cdot \frac{\lambda \cdot dx}{c_p \cdot m} \cdot \Delta t \quad (1)$$

Solving this equation for the whole domain, the heat flux in the sliced workpiece can be calculated. The simulation step time  $\Delta t$  is a fraction of the time for a tool rotation. This allows to consider the effect of heat input and propagation for every

single tooth engagement. To model the material removal by the process, the matrix  $A$  is recoded binary and the heat quantities of the removed elements from matrix  $Q$  are deleted. Therefore, the rotational movement of the cutting edge is approximated on the grid of the domain. For every rotation of the tool, the approximated movement of the edge is shifted by the feed per tooth  $f_z$  in the feed direction and the machined material is removed from the domain.

The heat input is modeled by a mathematical description of the process. For the localization of the heat input, the movement of the cutting edge is approximated. In one simulation step of the tool rotation, the generated heat is added to the elements of the Matrix  $Q$  next to the approximated cutting edge. Further, the heat flux in the workpiece is calculated until the next cutting edge engagement is reached (Fig. 3).

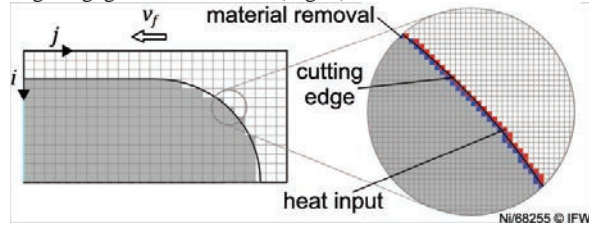


Fig. 3. Approximated material removal and heat input

After the simulation of the whole process the temperature at the measured surface is extracted from the simulation. An inverse method was used for the determination of the heat input. Therefore the temperature distribution at the measured surface is compared to the simulated temperatures. The heat input of the simulation is varied until measured and simulated temperatures coincides.

## 4. Results

### 4.1. Process stability

Fig. 4 shows the resulting chatter amplitude  $A_c$  in the frequency domain if chatter occurred. At the top diagram, the spindle speed is constant and the feed per tooth is varied.

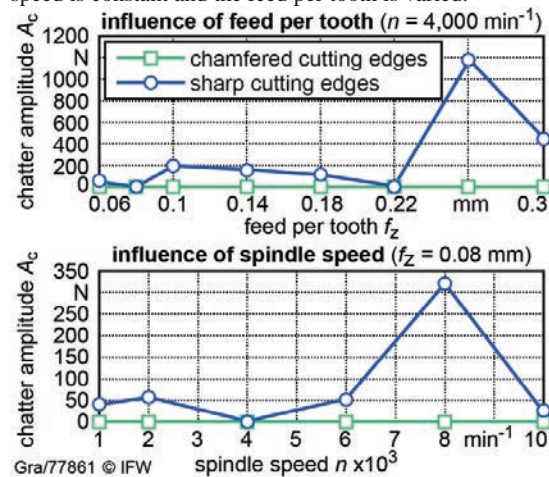


Fig. 4. Intensity of chatter vibrations

The bottom diagram has a constant feed per tooth and varying spindle speeds. For all investigated sets of process parameters, the end mill with chamfered cutting edges always led to a stable cutting operation. Thus, the amplitude is always zero. For the tool with a sharp cutting edge, the process was unstable in most cases. On the resulting finish surface, the difference are even more obvious (Fig. 5). It also shows that the process for the end mill with sharp cutting edges is stable at the beginning, but becomes unstable at some point during the process like in the most investigated milling operations.

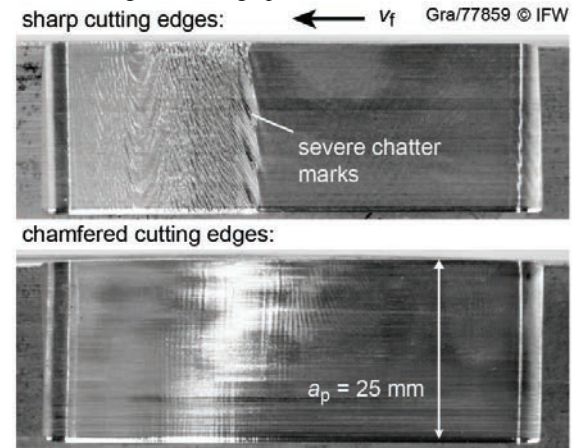


Fig. 5. Comparison of surface finish ( $n = 6,000$  min $^{-1}$ ,  $f_z = 0.08$  mm)

### 4.2. Heat generation

The black covered area, as seen in Fig. 1, is approx. 5,000 mm $^2$ . Based on the resolution of the thermal imaging camera and the distance to the workpiece, this area equals approx. 5,000 pixels. Thus, for every frame 5,000 temperature spots are measured. This means that in one second, considering a frame rate of 30 fps, 150,000 temperature spots are measured.

For the heat evaluation the main value of the 1,000 highest measured temperature spots was calculated for all investigated process parameters (Fig. 6). For the end mill with sharp cutting edges, the maximum temperature is below 100°C for all experiments. For the end mill with chamfered cutting edges, the maximum temperature values are much higher. This is an effect of the increased contact of the chamfered flank face and the wavy just cut workpiece surface. The induced additional force is obviously transformed into heat. The lower diagram in Fig. 6 shows that for low spindle speeds the maximum temperature is greatly reduced in comparison to higher spindle speeds, as might be expected. However, for the highest investigated spindle speeds at 8,000 min $^{-1}$  and 10,000 min $^{-1}$ , a slight temperature decrease can be observed. A possible explanation is that the contact between the chamfered flank face and the wavy surface depends on the length and amplitude of the sinusoidal waviness. High spindle speeds increase the wavelength, which leads to a decreased contact between tool and workpiece in the chamfer area [6].

The influence of the feed per tooth is shown in the upper diagram of Fig. 6. For the tool with chamfered flank faces, a tendency of a decreasing maximum temperature with



increasing feed per tooth values can be observed. With higher  $f_z$ , less heat can be transferred at the corresponding position spot, thus temperature decreases. The fluctuations of the maximum temperature in the diagram might be caused by different contact conditions between the wavy surface and the chamfered area. Additional experiments are required for a more accurate analysis. Generally, it can be stated that high feed per tooth is required when machining with chamfered cutting edges in order to reduce the risk of the emergence of soft spots.

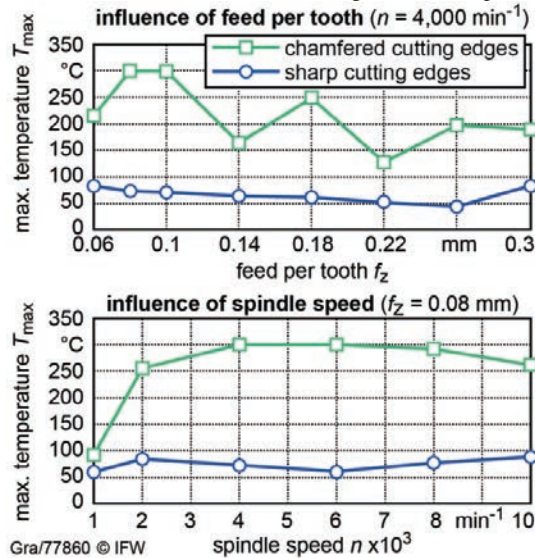


Fig. 6. Highest measured temperatures during experiments (max.: 300°C)

For a detailed investigation of the temperature distribution in the workpiece, simulations of selected processes were carried out. Fig. 7 shows the temperature distribution at different time steps ( $t_1 - t_7$ ) of a representative process. Initially, the temperatures in the workpiece are low. Due to the heat input and heat buildup in the direction of the feed, the temperatures rises until a steady state around the tool is reached. Further, it can be seen that the temperature difference between the machined side and the back side of the workpiece are low.

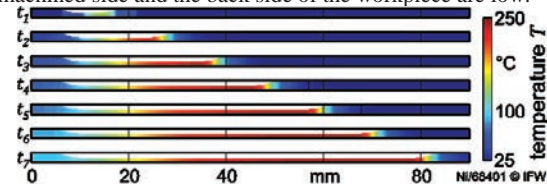


Fig. 7. Simulated temperature distribution in sliced workpiece (chamfered tool,  $f_z = 0.18 \text{ mm}$ ,  $n = 4,000 \text{ min}^{-1}$ )

Additionally, Fig. 8 shows the comparison of several time dependent maximum temperatures of the workpiece. The measured and simulated temperatures correlate well. Only a temperature peak at the end of the process is not reached in the simulation. The comparison of temperatures at the machined and the backside of the workpiece show that the temperature difference in the thin wall is low. Only directly after the tool engagement, the temperature at the machined side of the

workpiece is about 70°C higher. Until the beginning of the next tool engagement this temperature difference is balanced.

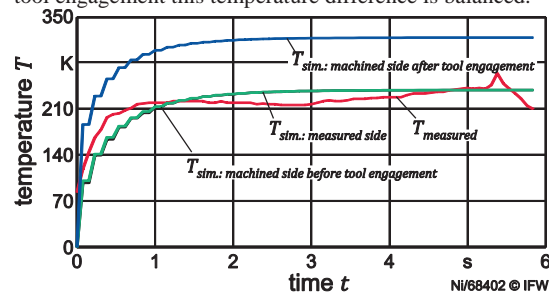


Fig. 8. Maximum temperature (chamfered tool,  $f_z = 0.18 \text{ mm}$ ,  $n = 4,000 \text{ min}^{-1}$ )

## 5. Conclusion

In the present research, the influence of chamfered cutting edges on stability and heat generation was investigated. It was shown that chamfered cutting edges in comparison to sharp cutting edges increase stability in milling of thin-walled workpieces. However, compared to sharp cutting edges, chamfered cutting edges have a much higher heat generation in the workpiece. For aluminum alloys, this yields a risk of soft spot forming. It was shown that by increasing the feed per tooth the maximum temperature in the workpiece could be reduced.

## Acknowledgements

This work has been funded by the Ministry of Economics, Labour and Transport of Lower Saxony within the project “Innoflex” (ZW3-80134969) and by the DFG within the research project “Thermomechanical Deformation of Complex Workpieces in Drilling and Milling Processes” (DE 447/90-2) within the DFG Priority Program 1480. The authors would like to thank the federal state of Lower Saxony and the DFG for their financial and organizational support of these projects.

## References

- [1] Airbus Global Market Forecast 2014 - 2033, Toulouse; 2014.
- [2] Chang JY, Lai GJ, Chen, MF. A study on the chatter characteristics of the thin wall cylindrical workpiece. In: International Journal of Machine Tools and Manufacture 34, No. 4; 1994. p. 489–498.
- [3] Tobias SA, Fishwick W. Eine Theorie des regenerativen Ratterns an Werkzeugmaschinen. In: Maschinenmarkt 17; 1956. p. 15–30.
- [4] Andrew C, Tobias SA. A critical comparison of two current theories of machine tool chatter. In: International Journal of Machine Tool Design and Research 1, No. 4; 1961. p. 325–335.
- [5] Sellmeier V, Denkena B. High speed process damping in milling. In: CIRP Journal of Manufacturing Science and Technology 5, No. 1; 2012. p. 8–19.
- [6] Wu DW. A new approach of formulating the transfer function for dynamic cutting process. In: ASME - Journal of Engineering for Industry 111; 1989. p. 37–47.
- [7] Weinert K. Trockenbearbeitung und Minimalmengenkühschmierung. Berlin: Springer; 1999.
- [8] Davis JR. Aluminium and aluminium alloys 2nd ed; 1994.
- [9] Grzesik W, Bartoszuk M, Nieslony P. Finite difference analysis of the thermal behaviour of coated tools in orthogonal cutting of steels. In: International Journal of Machine Tools and Manufacture, 44, No.14; 2004. p. 1451–1462.